

Supplementary Materials for

High-performance 3D printing of hydrogels by water-dispersible photoinitiator nanoparticles

Amol A. Pawar, Gabriel Saada, Ido Cooperstein, Liraz Larush, Joshua A. Jackman, Seyed R. Tabaei, Nam-Joon Cho, Shlomo Magdassi

Published 1 April 2016, *Sci. Adv.* **2**, e1501381 (2016)
DOI: 10.1126/sciadv.1501381

The PDF file includes:

- Detailed Materials and Methods
- Biocompatible studies with PI nanoparticles and 3D printed hydrogels.
- Determination of 3D printed hydrogel water content.
- Determination of 3D printed hydrogel mechanical strength.
- Fig. S1. Effect of storage temperature and duration on size of TPO nanoparticles.
- Fig. S2. Cryo-TEM image of an aqueous dispersion [0.1%(w/w)] of powder containing 25%(w/w) TPO.
- Fig. S3. Stability of TPO in an aqueous dispersion [1.6% (w/w)] of spray-dried powder at different time intervals after filtration through 0.22- μm PVDF filters.
- Fig. S4. X-ray diffraction patterns for spray-dried powders containing TPO nanoparticles after 85 days of storage at 25°C.
- Fig. S5. Polymerization kinetics.
- Fig. S6. Effects of TPO nanoparticle concentration on cell viability.
- Fig. S7. Relative cell viability of Huh7 liver cells cultured on different substrates.
- Fig. S8. Mechanical characterization of polyacrylamide hydrogel fabricated with TPO nanoparticles.
- Table S1. Composition [% (w/w)] of the microemulsions before spray drying.
- Table S2. Theoretical composition [in % (w/w)] of the spray-dried powders.
- Table S3. Molar extinction coefficients of TPO nanoparticles and I2959 at standard center wavelengths of light sources used for DLP-based 3D printers.
- Table S4. Summary of different light sources used for hydrogel formation.
- Table S5. Summary of photopolymerization results using different water-soluble PIs with aqueous acrylamide solutions in air at 25°C.
- References (42–64)

Supplementary Materials

S1. Supplementary Materials and Methods

Materials

N-butyl acetate (nBuAc; $\geq 99.5\%$), 2-propanol (IPA; $\geq 99.5\%$), sodium dodecyl sulfate (SDS; $\geq 98.5\%$), acrylamide ($\geq 99\%$) and polyvinylpyrrolidone (PVP; MW 40,000) were purchased from Sigma-Aldrich, St. Louis, USA. 2,4,6-trimethylbenzoyl-diphenylphosphine oxide (TPO; Igracure TPO) was obtained from BASF, Kasiten, Germany. Polyethylene glycol (600) diacrylate (SR-610) and ethoxylated trimethylolpropane triacrylate, (SR-9035) were obtained from Sartomer-Akrema, Colombes Cedex, France. Yellow dye (Duasyn Acid Yellow XX-SF) was purchased from Clariant, Frankfurt, Germany. Ultrapure water obtained from NANOpure®-Diamond™, (TDW; $0.0055 \mu\text{S}\cdot\text{cm}^{-1}$; Barnsted system, Dubuque, IA, USA) was used in all the experiments.

Preparation of photoinitiator containing microemulsions

Our previously reported method to prepare nanoparticles of a poorly water-soluble by evaporation of volatile oil-in-water microemulsions, was used to prepare the photo-initiator nanoparticles (33). N-butyl acetate (nBuAc) was selected as the volatile solvent forming the microemulsion droplets, since TPO is readily soluble in nBuAc (25 %w/w) at room temperature. O/W microemulsions containing varying concentrations of TPO were prepared at room temperature by mixing nBuAc with SDS (as surfactant), IPA (as co-solvent) and PVP (as crystallization inhibitor) to create an "oil" (organic) phase in which TPO is dissolved. Afterward the oil phase was mixed with TDW and magnetically stirred at 25 °C until clear systems were obtained. The microemulsions compositions are presented in Table S1.

Converting the microemulsion into nanoparticles

The above microemulsions were spray dried by a Mini Spray Dryer B-290 equipped with inert loop dehumidifier B-296 (Buchi, Flawil, Switzerland). Process conditions were: air inlet temperature 120 °C (± 2 °C), drying chamber (outlet) temperature 60 °C (± 2 °C), liquid introduction rate $5 \text{ mL}\cdot\text{min}^{-1}$, spray flow rate $414 \text{ norml}\cdot\text{h}^{-1}$, aspirator rate $35 \text{ m}^3\cdot\text{h}^{-1}$, nitrogen pressure 6 atmospheres. The resultant products were dry free flowing powders (compositions given in Table S2), which were stored in tightly closed glass vials.

Similar powders were also obtained by lyophilization of microemulsions. Lyophilization was performed using laboratory-scale benchtop freeze-drying system (Labconco Freezone 2.5, Missouri, USA). Before

lyophilization, microemulsions (30 mL sample in a 100 mL round bottom flask) were freeze-dried in a bath of liquid nitrogen for 5 minutes. Then lyophilized at a temperature of $-47 \pm 3^\circ\text{C}$ and absolute pressure of ~ 0.470 mbar. The samples were kept in those conditions for 24 hours.

TPO nanoparticles dispersion in water

The powders obtained at the end of the spray drying process were dispersed (0.1-1 % w/w) in TDW. The samples were vortexed for 1 min and magnetically stirred at room temperature for 5 min. This powder dispersing procedure was performed in order to have a reproducible procedure, although simple manual shaking of the dispersion for 1–2 min was sufficient to obtain a clear system.

Control TPO solubilization experiments were performed to validate the necessity of preparing TPO nanoparticles. Possible solubilization was evaluated by dispersing bulk TPO in aqueous solution of SDS and PVP concentrations similar to those of components in 1 % w/w aqueous dispersion of TPO nanoparticles (TPO 0.05 %, SDS 0.475 %, PVP 0.475 % and water 99%). The mixture was then subjected to either high speed stirring (1000 rpm) for 24 hours at room temperature or sonication for 60 minutes, followed by filtration using a 0.22 μm filter and measurements of the concentration of solubilized TPO by UV spectrophotometer.

Particle size measurements of TPO nanoparticles

The particle size distribution after dispersion in water was measured at room temperature by dynamic light scattering using a Nano-ZS Zetasizer (Malvern, Worcestershire, UK). The instrument is equipped with a 633-nm laser, and the light scattering is detected at 173 degrees by a backscattering technology (non-invasive backscatter). The measurements were performed in triplicate for each sample after dispersion of the powder in water.

Cryogenic-transmission electron microscopy

After dispersing the powder in water (0.1-1 %w/w), the TPO nanoparticles were evaluated by Cryo-TEM. A 3 μL drop of the dispersion was placed on a Lacey carbon film supported on a TEM copper grid (Ted Pella, Ltd.) held by tweezers inside a controlled-environment vitrification system (Vitrobot Mark IV, FEI). The excess liquid was blotted with a filter paper, resulting in the formation of thin sample films within the micropores in the perforated carbon layer supported on the grid. The specimen was then plunged into a reservoir of liquid ethane pre-cooled by liquid nitrogen, to ensure its vitrification and to prevent ice crystal formation. The vitrified specimen was transferred under liquid nitrogen to a Gatan 626 cryogenic sample holder, cooled to -177°C . All samples were studied under

low dose conditions in a FEI Tecnai 12 G2 TEM, operated at 120 kV. Images were recorded on a 4K x 4K FEI Eagle CCD camera.

Crystallinity measurement of TPO nanoparticles

Powder X-ray diffraction (PXRD) measurements were performed using the D8 Advance diffractometer (Bruker AXS, Karlsruhe, Germany) with a goniometer radius of 217.5 mm, secondary graphite monochromator, 2° Soller slits, and 0.2 mm receiving slit. Low background quartz sample holders were carefully filled with the samples. The specimen weight was approximately 0.2 g. PXRD patterns within the range of 5° to 35° 2 θ were recorded at room temperature using CuK α radiation ($\lambda = 1.5418 \text{ \AA}$) with the following measurement conditions: tube voltage of 40 kV, tube current of 40 mA, step-scan mode with a step size of 0.02° 2 θ , and counting time of 1 s per step

UV absorption measurements

In order to evaluate the suitability of the TPO nanoparticles for aqueous ink formulations, we further studied the stability of the aqueous dispersion was quantified by UV spectroscopy. The stability of dispersed photoinitiator nanoparticles in water was evaluated by measuring the TPO concentration in the filtrate at various time intervals after dispersing the powders in water. Photoinitiator nanoparticles were dispersed in water and subsequently filtered through 0.22 μm PVDF filters. Hydrophobic PVDF filters were selected for low absorption of aqueous dispersions. Quantification of TPO concentration in the filtrate was done by UV spectrophotometer (UV-1800, Shimadzu, Kyoto, Japan). A standard absorbance-concentration calibration curve was attained for TPO dissolved in isopropanol-water (1:1) mixture. The absorbance of sample solutions was recorded using UV-vis spectrometer (UV-1800, UV probe 2.43; Shimadzu, Kyoto, Japan). The experiments indicated that the dispersion remains stable for at least 50 days (Fig. S3), and therefore can be used for the ink formulation.

The molar extinction coefficients (ϵ) were measured and compared with commercially available photoinitiator I2959. Molar extinction coefficients for TPO nanoparticles and I2959 were determined from the absorbance of 4 mM photo-initiator solutions in water. Absorption spectra were determined in the range of 300–440 nm, as this range reflects the emission of most commercially available UV lamps.

Measurement of photoinitiator activity

To determine the polymerization efficiency of TPO nanoparticles, polymerization kinetics of acrylamide in aqueous solutions with TPO nanoparticles was measured and compared to that of aqueous solutions of the commercial water-soluble photoinitiator I2959. Fourier Transform Infrared Spectrophotometer (ALPHA FT-IR Spectrometer, Bruker) was used in conjunction with platinum ATR single reflection

diamond accessory (Sample scans 64; Resolution 4 cm⁻¹). Measured data was analyzed using Analytical Data System for FTIR (OPUS 6.5, Bruker). The polymerization solutions comprised aqueous solutions containing 20 %w/w monomer (acrylamide) with cross-linking monomer polyethylene glycol 600 diacrylate (5 % w/w of the monomer) and photoinitiator (TPO nanoparticles or Igracure 2959 at concentration of 0.5 % w/w of the monomer) were used.

Measurements were performed on ~200 µl of polymerization solution dropped on the ATR diamond. The UV light was radiated onto the sample through a chamber (at 1.5 cm height) centered at the ATR diamond. Monochromatic UV LED (Integration Technology, Oxfordshire, UK) irradiating at 395 nm was used for photo-curing. IR spectra were recorded after every 4 seconds, for a total duration of 40 seconds. Each spectrum was the Fourier transformation of 64 scans collected over the spectral range of 1800-800 cm⁻¹ with instrument resolution of 4 cm⁻¹.

The polymerization kinetics of acrylamide was calculated from the decay/disappearance of the absorption peaks of methylene group vibrations at 988 cm⁻¹ (assigned to out-of-plane bending mode of the =C-H unit) normalized to the C=O stretching peak at 1654 cm⁻¹ as an internal standard (39). The conversion rate (CR) was calculated using Equation. 2, where $A_{monomer}$ and A_{Std} are absorbance of monomer (from IR peak of 988 cm⁻¹) and internal standard (from IR peak of 1654 cm⁻¹), respectively, at beginning of polymerization reaction (0) and after different time intervals (t) (39)

$$CR = 1 - \frac{(A_{monomer} / A_{Std})_t}{(A_{monomer} / A_{Std})_0} \quad (1)$$

S2. Biocompatible studies with PI nanoparticles and 3D printed hydrogels

To determine biocompatibility of the photoinitiator nanoparticles, cytotoxicity experiments were performed following an adapted protocol from Ovsianikov et al. (42). MRC-5 human fibroblasts were seeded onto a 96-well tissue culture plate at a density of 5×10^3 cells per well in Alpha MEM (HyClone) medium supplemented with 10% FBS and 1% Streptomycin/Amphotericin B/Penicillin. Photoinitiator (PI) was dissolved in 1× PBS to a final concentration 10% w/w. The solution was filtered for sterilization. Two-fold dilution series of the 10% PI solution was prepared in the medium to obtain the range of concentrations: 0.04% - 5% w/w. After removing the medium, the PI solution was added to the cells, and the plate was incubated for 30 min at 37 °C. Cells in medium (no PI added) were used as a negative control. Triton X-100 (1%) was used to achieve 100% cell cytotoxicity (positive control). All

steps were performed without direct exposure to light. The PI solution was removed, and cells were washed twice with PBS. Fresh medium was then added to the cells, and after 24 h incubation at 37 °C, cell viability was determined with the CCK-8 kit. Fibroblasts were incubated with CCK-8 solution containing WST-8* for 90 minutes. WST-8 is reduced by dehydrogenases in the cells, giving formazan, which was detected by absorbance spectrometry measurements at 450 nm. Viability of the cells was calculated as percentage of the cells that remained live after addition of the PI. As shown in Fig.S6, cell viability was sufficiently maintained, 91% and 66% for 0.05% and 0.2% w/w of TPO nanoparticles powder, respectively.

To determine biocompatibility of 3D printed hydrogels, cell-viability experiments were performed following an adapted protocol from Dyondi et al.(43). For the cell seeding experiments, Huh7 liver cells were seeded onto the hydrogel scaffold surfaces at a density of 5×10^3 cells per well in Alpha MEM (HyClone) medium supplemented with 10% FBS and 1% Streptomycin/Amphotericin B/Penicillin. Cells on conventional polystyrene plates were used as a negative control and Triton X-100 (1%) was used to achieve 100% cell cytotoxicity (positive control). After 24 h incubation at 37 °C, viability of the seeded cells was determined with the CCK-8 kit. The Huh7 liver cells were incubated with CCK-8 solution containing WST-8* for 90 minutes. WST-8 is reduced by dehydrogenases in the cells, giving formazan, which was detected by absorbance spectrometry measurements at 450 nm. Viability of the cells was calculated as percentage of the cells that remained live after addition of the PI. As shown in Fig. S7 we found that cell viability on the polyacrylamide scaffold prepared with the TPO nanoparticles was comparable, 80% viability, to the commonly used poly(ethylene glycol) diacrylate (PEG-DA, 20 %w/w) hydrogel scaffold as the reference case.

S3. Determination of 3D printed hydrogel water content

In order to measure the water content of the hydrogel, the printed samples were immersed in deionized water for 24 h at room temperature in order to reach equilibrium swelling. Then, the hydrogels were removed from the aqueous medium and blotted dry in order to gently remove excess water. The swollen hydrogel mass was recorded. Afterwards, the hydrogels were placed in a freeze-dryer for 24 h in order to remove all water content and then the dry mass was recorded. The water mass fraction was determined from the ratio of the dry and swollen masses. The measured value of the water content in the hydrogel was determined to be 84.1 ± 1.5 % w/w ($n = 6$).

S4. Determination of 3D printed hydrogel mechanical strength

The viscoelastic properties of the printed hydrogels were characterized using steady shear and sinusoidal shear rheometry (Fig. S8). Frequency-sweep measurements were conducted using an Anton Paar

Physica MCR 501 rheometer equipped with a Peltier plate temperature-controlled base with a parallel plate with 10 mm diameter. The testing conditions for all measurements were 0.1 % strain amplitude at an oscillation frequency of 0.02–0.1 Hz within the linear viscoelastic regime. The complex shear modulus was then calculated by the following relation: $G^* = [(G')^2 + (G'')^2]^{1/2}$, where G' = shear storage modulus and G'' = shear loss modulus. Based on this approach, we determined the complex modulus of the 3D-printed polyacrylamide hydrogel to be 47.3 ± 0.7 kPa. This value is more than six-times greater than the complex modulus of a reference hydrogel sample (20% w/w PEG-DA) that was measured in parallel. Considering the high water fraction mentioned above and the strong mechanical properties, the 3D-printed polyacrylamide hydrogel has attractive features that could be further optimized for specific applications.

S5. Supplementary Figures

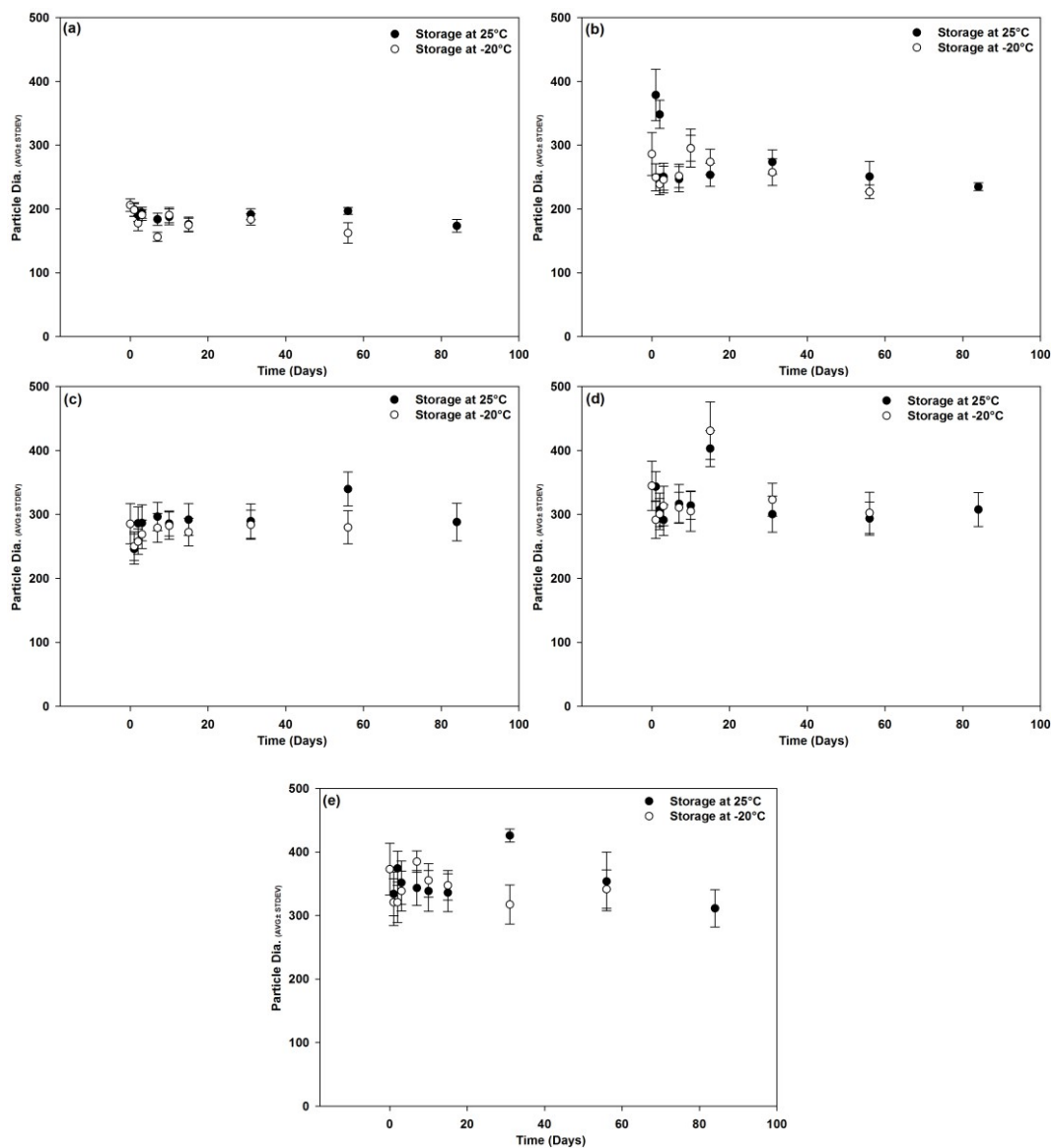


fig. S1. Effect of storage temperature and duration on size of TPO nanoparticles. (A to E) Mean size of TPO nanoparticle containing varying TPO concentrations (A) 5 % w/w, (B) 10 %w/w, (C) 15 %w/w, (D) 20% w/w and (E) 25 % w/w

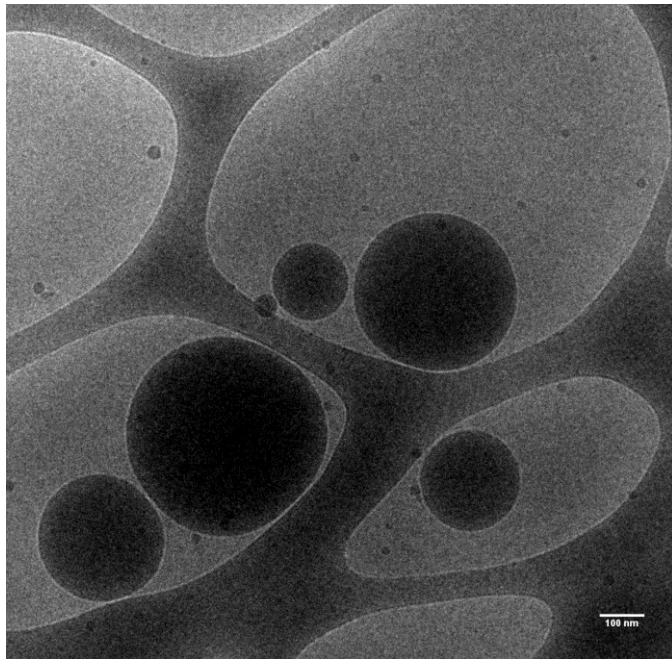


fig. S2. Cryo-TEM image of an aqueous dispersion [0.1% (w/w)] of powder containing 25 % (w/w) TPO.

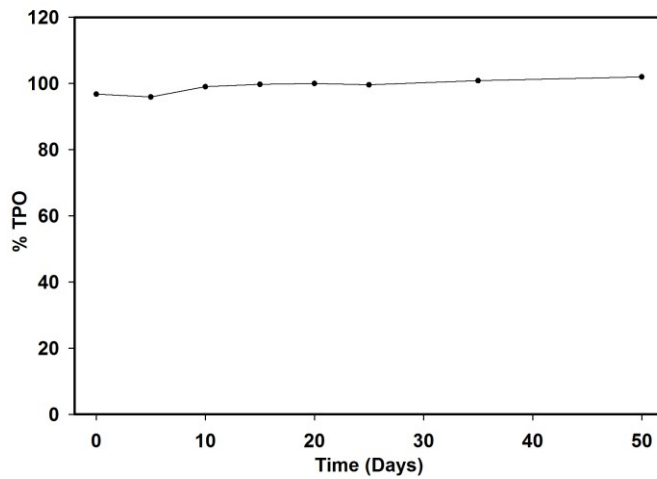


fig. S3. Stability of TPO in an aqueous dispersion [1.6% (w/w)] of spray-dried powder at different time intervals after filtration through 0.22- μm PVDF filter.

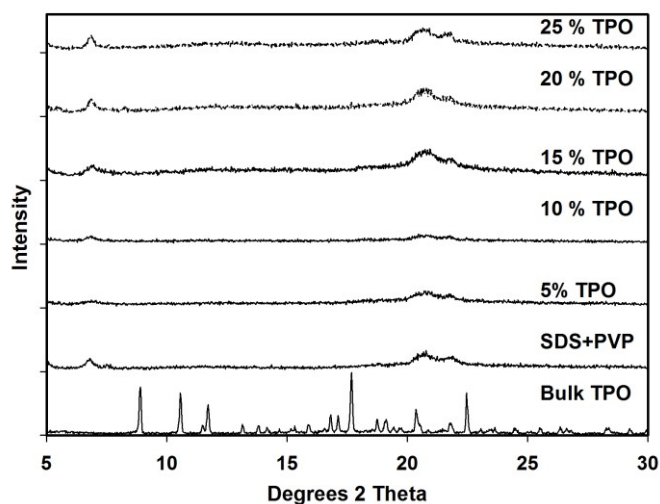


fig. S4. X-ray diffraction patterns for spray-dried powders containing TPO nanoparticles after 85 days of storage at 25°C.

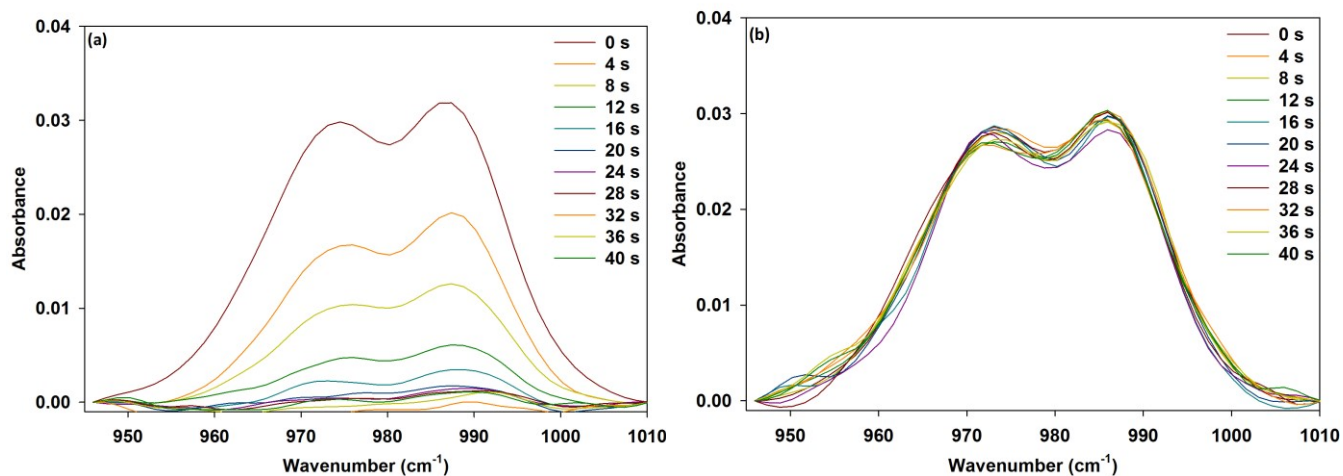


fig. S5. Polymerization kinetics. (A to B) Fourier transform infrared spectrum of acrylamide aqueous solutions with (a) TPO nanoparticles and (b) Irgacure 2959 acquired after every 4 seconds of UV exposure over the entire duration (40 seconds).

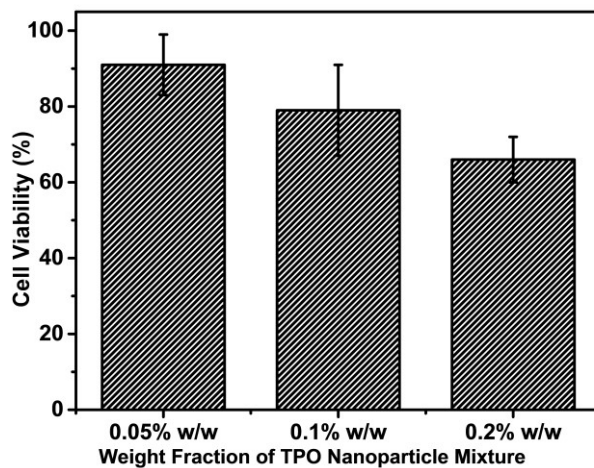


fig. S6. Effects of TPO nanoparticle concentration on cell viability. 5×10^3 cells/well were incubated with varying concentrations of TPO nanoparticles for 30 min and then the TPO nanoparticle was washed away. After 24 h additional incubation at 37 °C, the cell viability was measured on the basis of dehydrogenase activity, as determined by spectroscopic detection of the formazan product. The cell viability percentage was calculated based on a control sample without TPO nanoparticle.

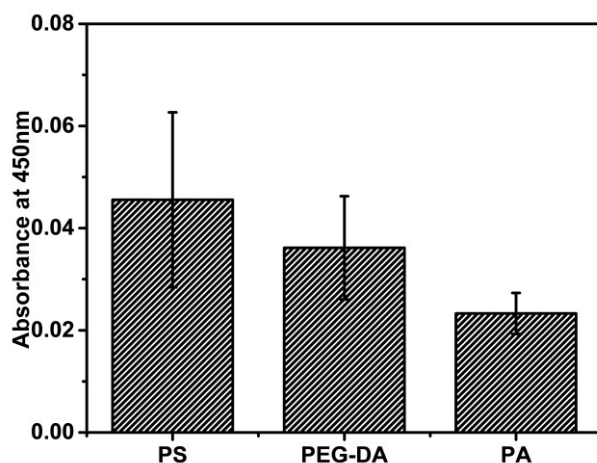


fig. S7. Relative cell viability of Huh7 liver cells cultured on different substrates. 5×10^3 cells were seeded on top of the test polyacrylamide (PA) hydrogel or control materials, a polystyrene (PS) substrate or poly(ethylene glycol) diacrylate (PEG-DA) hydrogel. After 24 h incubation at 37 °C, the cell viability was measured on the basis of dehydrogenase activity, as determined by spectroscopic detection of the formazan product.

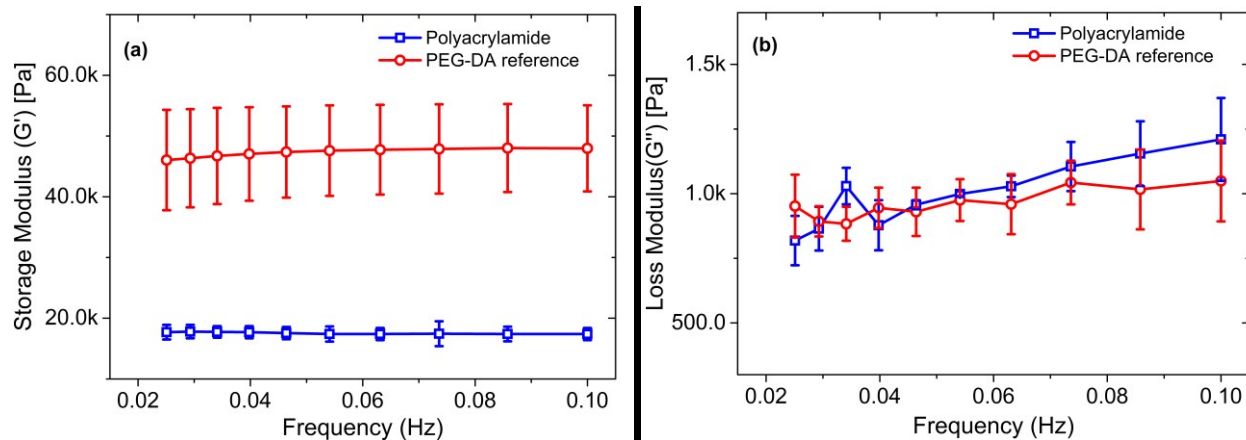


fig. S8. Mechanical characterization of polyacrylamide hydrogel fabricated with TPO nanoparticles. (a) Storage modulus and **(b)** loss modulus of the fabricated hydrogel were recorded as functions of the oscillation frequency. The reference case consisted of a 20% w/w PEG-DA hydrogel sample prepared by conventional means.

S6. Supplementary Tables

Table S1. Composition [% (w/w)] of the microemulsions before spray drying.

S. No.	TPO	nBuAc	IPA	SDS	PVP	TDW
1	0	24	21.0	7.5	7.5	40
2	0.8	23.2	21.0	7.5	7.5	40
3	1.7	22.3	21.0	7.5	7.5	40
4	2.6	21.4	21.0	7.5	7.5	40
5	3.8	20.3	21.0	7.5	7.5	40
6	5.0	19.0	21.0	7.5	7.5	40

Table S2. Theoretical composition [in % w/w] of the spray-dried powders.

S. No.	TPO	SDS	PVP
1	0	50	50
2	5	47.5	47.5
3	10	45	45
4	15	42.5	42.5
5	20	40	40
6	25	37.5	37.5

Table S3. Molar extinction coefficients of TPO nanoparticles and I2959 at standard center wavelengths of light sources used for DLP-based 3D printers.

	365 nm	385 nm	395 nm	405 nm
TPO Nanoparticles	659.9	602.1	416.6	200.3
I2959	2.3	0.1	0.0	0.0

Table S4. Summary of different light sources used for hydrogel formation.

S.No.	Light source wavelength	Light Source Details	Hydrogel formation process	Reference
1	305	Benchtop UV transilluminator	Petri dishes in chamber	(44)
2	325	He–Cd laser	Petri dishes in chamber	(45)
3	350	UVA lamp	Petri dishes in chamber	(46)
4	365	UV lamp	Petri dishes in chamber	(14)
5	365	UV lamp	Petri dishes in chamber	(47)
6	365	UV spot lamp	Petri dishes in chamber	(48)
7	365	UV lamp	Petri dishes in chamber	(49)
8	365	UV lamp	Extrusion based 3D printing	(50)
9		UV lamp	PSL apparatus+DLP	(51)
10	365	UV lamp	Bioforce Nano eNabler	(52)
11	515	Femtosecond laser emitting at ~515 nm	Two photon polymerization	(42)
12	780	Ti: sapphire laser emitting at 100 fs	Two photon polymerization	(53)
13	800	Ti: sapphire laser emitting at 100 fs	Two photon polymerization	(54)
14	N/A	UV spot lamp	SLA+DMD	(55)

Table S5 Summary of photopolymerization results using different water-soluble PIs with aqueous acrylamide solutions in air at 25°C.

S.No.	Photoinitiator	Polymerization Results			Reference
		Percent Conversion	Irradiation time	UV light source	
0	TPO nanoparticles	~80	15 s	LED 395 nm	Present work
1	Synthesized polymethylphenylsilane-co-poly(polyethyl-ene glycol acrylate)	~80	40 s	UV lamp (250 -365 nm)	(56)
2	Synthesized cyclodextrin and 5-thia pentacene-14-one complex	~50	900 s	400 W Mercury lamp	(57)
3	Synthesized benzophenone/methylate d-cyclodextrin inclusion complex with jeffamine based dendrimic co-initiator	~100	3600 s	UV lamp (350 nm)	(58)
4	Synthesized 2-thioxanthone-thioacetic acid sodium salts	~38	900 s	400 W Mercury lamp	(59)
5	Synthesized thioxanthone-based 2-(carboxymethoxy) thioxanthone	~16	900 s	400 W Mercury lamp	(59)
6	Synthesized thioxanthone polystyrene and methyl-diethanolamine	~80	240 s	400 W Mercury lamp	(60)
7	Synthesized phenacylpyridinium Oxalate	~22	1800 s	UV lamp (> 300nm)	(61)
8	Synthesized methylated beta-cyclodextrin and 2,2-dimethoxy-2-phenylacetophenone	~30	25 s	Hg lamp (365 nm)	(62)
9	Synthesized dendritic macrophotoinitiators containing thioxanthone	~50	3600 s	Not specified	(63)
10	2-oxoglutaric acid	~80	1800 s	Light source 313 nm	(64)